HAWC+ Observations of OMC-1

David T. Chuss
Villanova University
for the HAWC+ Science Team

SOFIA Tele-Talk, May 8, 2019

HAWC+ Science Team

- David Chuss
- B-G Andersson
- John Bally
- Jessie Dotson
- Darren Dowell
- Jordan A. Guerra
- Al Harper
- Martin Houde
- Terry Jones
- Alex Lazarian
- Enrique Lopez Rodriguez
- Joe Michail
- Mark Morris
- Giles Novak
- Javad Siah
- Johannes Staguhn
- John Vaillancourt
- Carrie Volpert
- Mike Werner
- Ed Wollack
- Dominic Benford
- Marc Berthoud
- Erin Cox
- Dick Crutcher
- Danny Dale
- Laura Fissel
- Paul Goldsmith
- Ryan Hamilton
- Shaul Hanany
- Thomas Henning
- Leslie Looney
- Harvey Moseley
- Fabio Santos
- Ian Stephens
- Kostantinos Tassis
- Christopher Trinh
- Eric Van Camp
- Derek Ward-Thompson

(Authors on Chuss+ 2019)

Star formation is an essential ingredient in our Origin Story

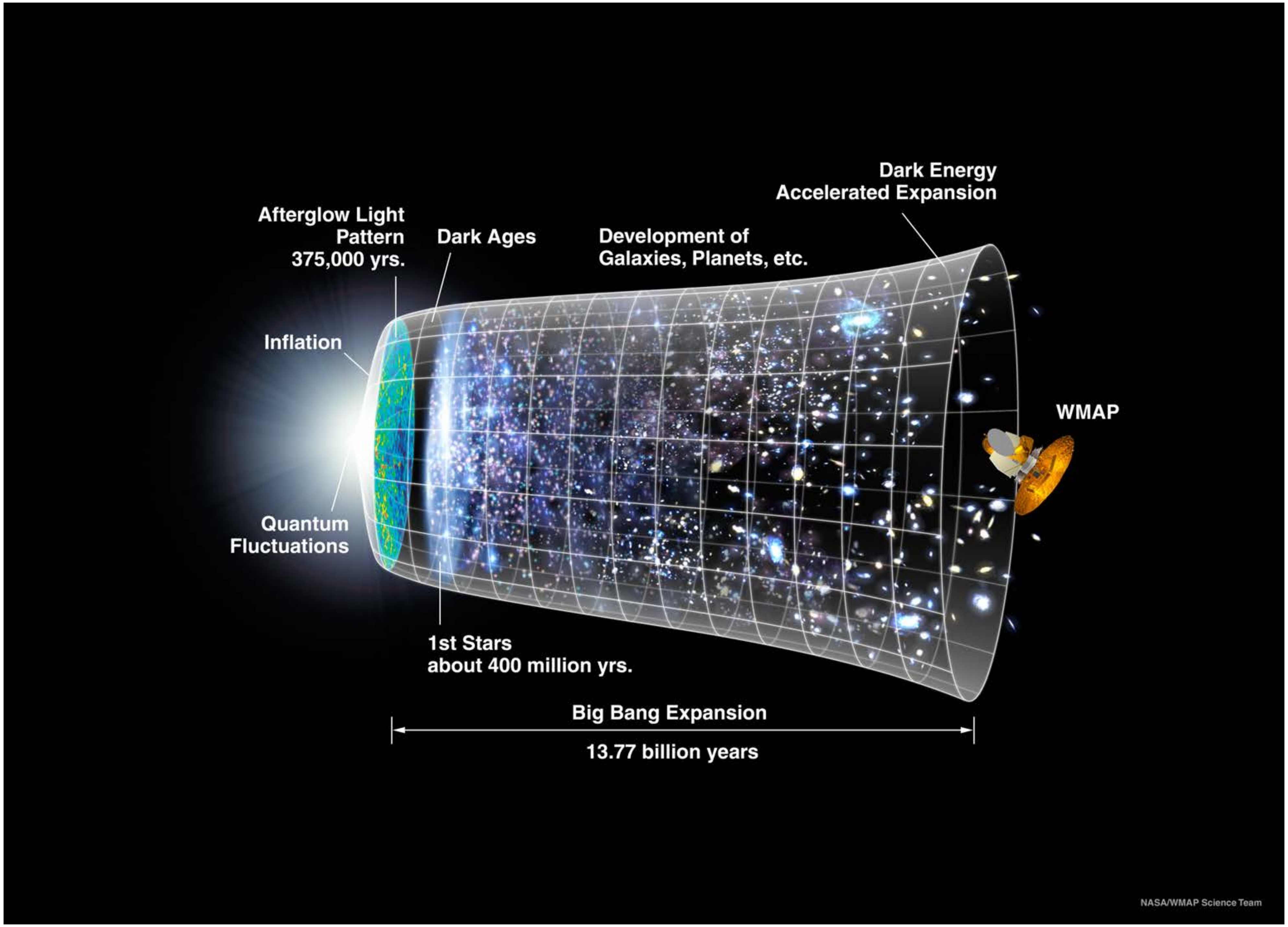

Talk Outline

- Introduction
  - Star formation
  - Dust polarization
  - SOFIA/HAWC+
- OMC-1 HAWC+ data
  - SEDs
  - Polarization data and general features
  - Polarimetry data cuts
  - Local Dispersion- grain alignment
  - Magnetic field strength- DCF technique
  - Implications for BN/KL Explosion
- Summary

Star Formation Rate

0.68-1.45 Solar Masses/Year
(Robitaille et al. 2010- cataloging properties of YSO’s)

This is extremely inefficient
(by a factor of up to 100; based on free-fall models alone)

Possibilities:

- Turbulence
- Feedback
- Magnetic Support

Background- Molecular Clouds

- Dust is coexistent with molecular phase in molecular clouds
- Dust Reprocesses optical starlight to IR (absorbs optical light, emits in the (F)IR)
- Magnetic fields are generally “frozen into” the material in molecular clouds.
- Polarized thermal emission from dust can be used to trace the magnetic field structure.

Grain Alignment

- Anisotropic radiation fields (ISRF) impart suprathermal rotation to grains ($a>0.1$ micron). This implies biattenuance to circular polarization (chiral grains).
- The grains become magnetized due to the Barnett effect (Some of the external angular momentum gets swapped for spin angular momentum of unpaired electrons).
- The magnetized grains precess around the Interstellar magnetic field.
- The grains preferentially spin about the axis of the greatest moment of inertia. (internal dissipative forces)
- Paramagnetic dissipation aligns the spin axis with the magnetic field.
- **UPSHOT: Polarized thermal emission from interstellar dust grains is perpendicular to the magnetic field as projected onto the plane of the sky.**

RAT; Dolginov & Mytrophanov 1976; Draine & Weingartner 1997; Lazarian & Hoang 2007

Why the Far-Infrared?

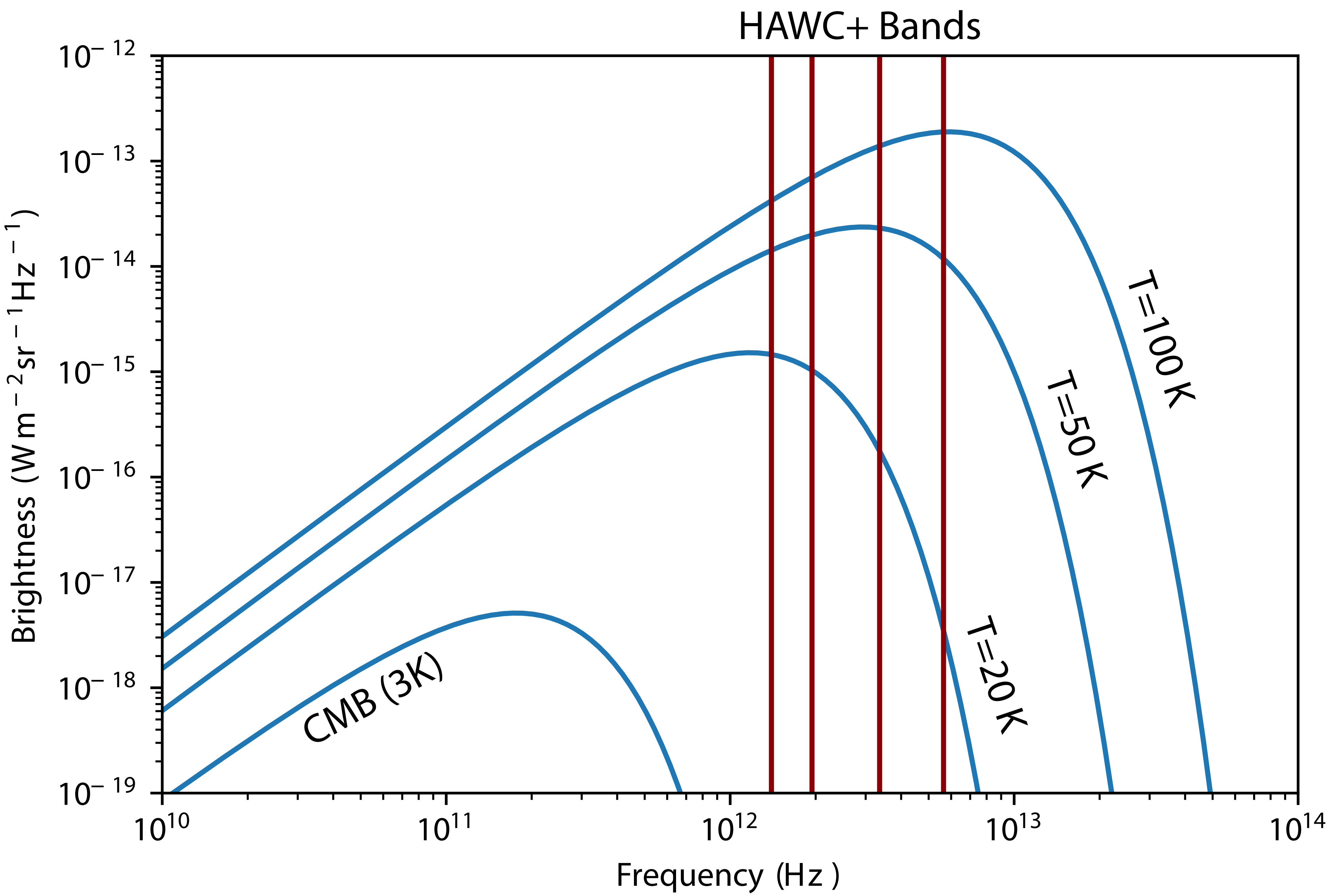

Tracing magnetic fields over a range of conditions in the ISM


SOFIA
STRATOSPHERIC OBSERVATORY
FOR INFRARED ASTRONOMY
NASA
DLR
N747NA

HAWC+ (High-resolution Airborne Wideband Camera+)

HAWC+ Specifications (Harper+ 2018)

Band name	Band center (microns)	FWHM Bandwidth (microns)	Pixel size (arcsec)	Beam size (arcsec FWHM)	Polarimetry field of view[a] (arcmin)	Photometry field of view[a] (arcmin)	Instantaneous point-source sensitivity[b] (Jy $s^{0.5}$)
A	53	8.7	2.55	4.85	1.4×1.7	2.8×1.7	1.9
B	62	8.9	4.02	(footnote c)	2.1×2.7	4.2×2.7	(footnote c)
C	89	17	4.02	7.8	2.1×2.7	4.2×2.7	2.2
D	154	34	6.90	13.6	3.7×4.6	7.4×4.6	2.0
E	214	44	9.37	18.2	4.2×6.2	8.4×6.2	1.7

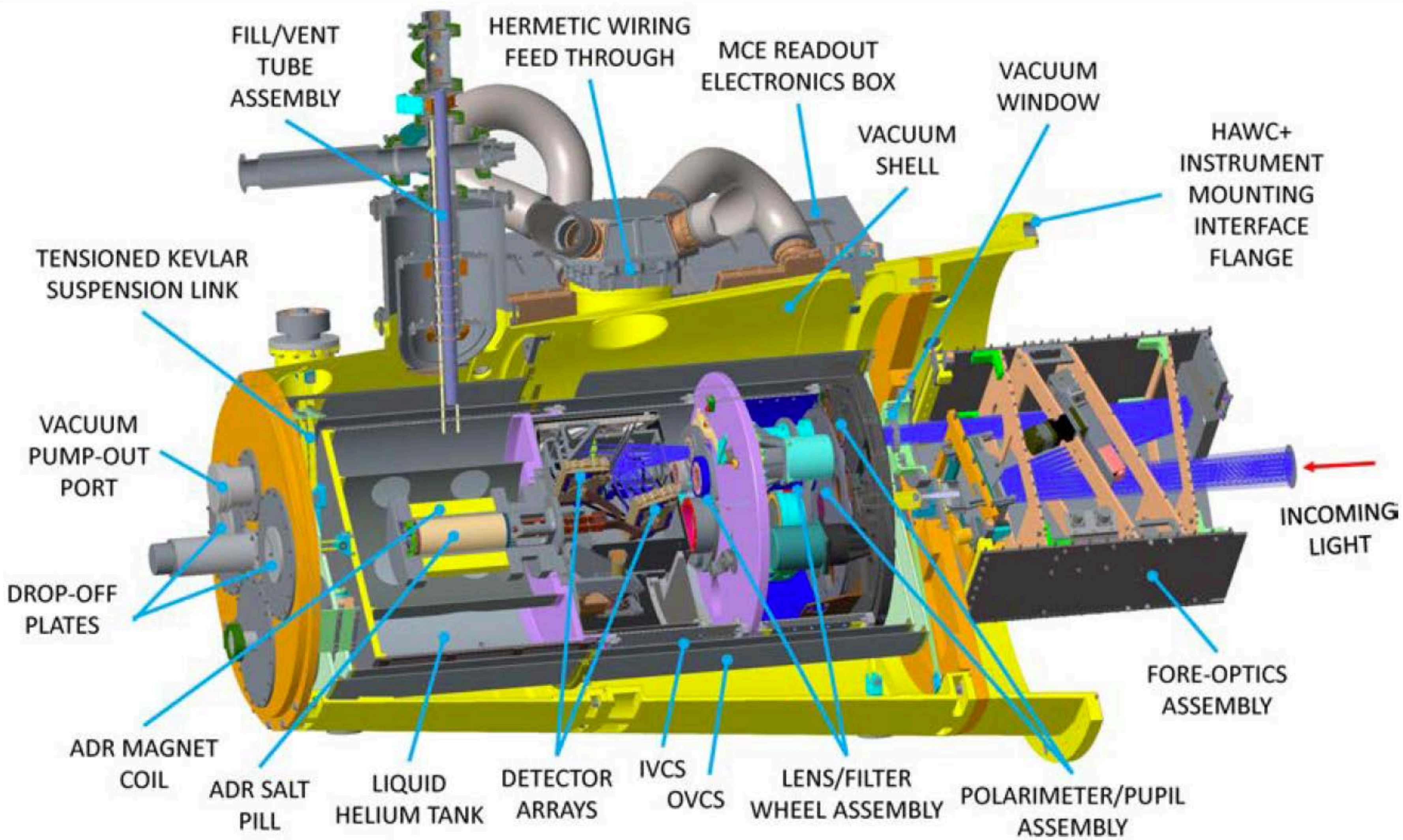

Stars form in Molecular Clouds: Ammonia as a tracer of dense gas

OMC-1

- Closest Sight of Massive star formation (~390 pc; Kounkel+ 2017)

WISE/GBT- R. Friesen, Dunlap Institute/J.Pineda, MPIP/GBO/AUI/NSF/NASA

Spectral Energy Distribution (SED) Determination

Free-free

$$I_{\text{ff}} = C\left(\frac{\nu}{30\ \text{GHz}}\right)^{-0.12}$$

Hensley+ (2015)

Dust

$$I_\nu = (1 - e^{-\tau(\nu)})B_\nu(T)$$

$$\tau(\nu) \equiv \varepsilon(\nu/\nu_0)^\beta$$

$$\varepsilon = \kappa_{\nu_0}\mu m_{\text{H}}\text{N}(\text{H}_2)$$

$$\kappa_{\nu_0}(1000\ \text{GHz}) = 0.1\ \text{cm}^2\ \text{g}^{-1}$$

$$\mu = 2.8$$

Data Sets- Table 2 (Chuss+2019)

Adopted Photometry Calibration Values

Observatory/ Instrument (⋯)	Wavelength (μm)	Beam Size FWHM (″)	Color Correction (⋯)	Color Correction Uncertainty (⋯)	Calibration Uncertainty (%)	Paper Reference (⋯)
SOFIA/HAWC+	53	5.1	⋯	⋯	15	This paper
SOFIA/HAWC+	89	7.9	⋯	⋯	15	This paper
SOFIA/HAWC+	154	14.0	⋯	⋯	15	This paper
SOFIA/HAWC+	214	18.7	⋯	⋯	20	This paper
Herschel/PACS	70	5.6	1.025	0.004	20	Abergel (2010)
Herschel/PACS	100	6.8	1.004	0.018	20	André (2007)
Herschel/PACS	160	11.3	0.929	0.027	20	André (2007)
Herschel/SPIRE	250	18.2	0.970	0.005	10	André (2011), Bendo et al. (2013)
JCMT/SCUBA-2	850	14.2	⋯	⋯	15	Mairs et al. (2016)
GBT/MUSTANG	3500	9.0	⋯	⋯	15	Dicker et al. (2009)
GBT and VLA	35000	8.4	⋯	⋯	15	Dicker et al. (2009)

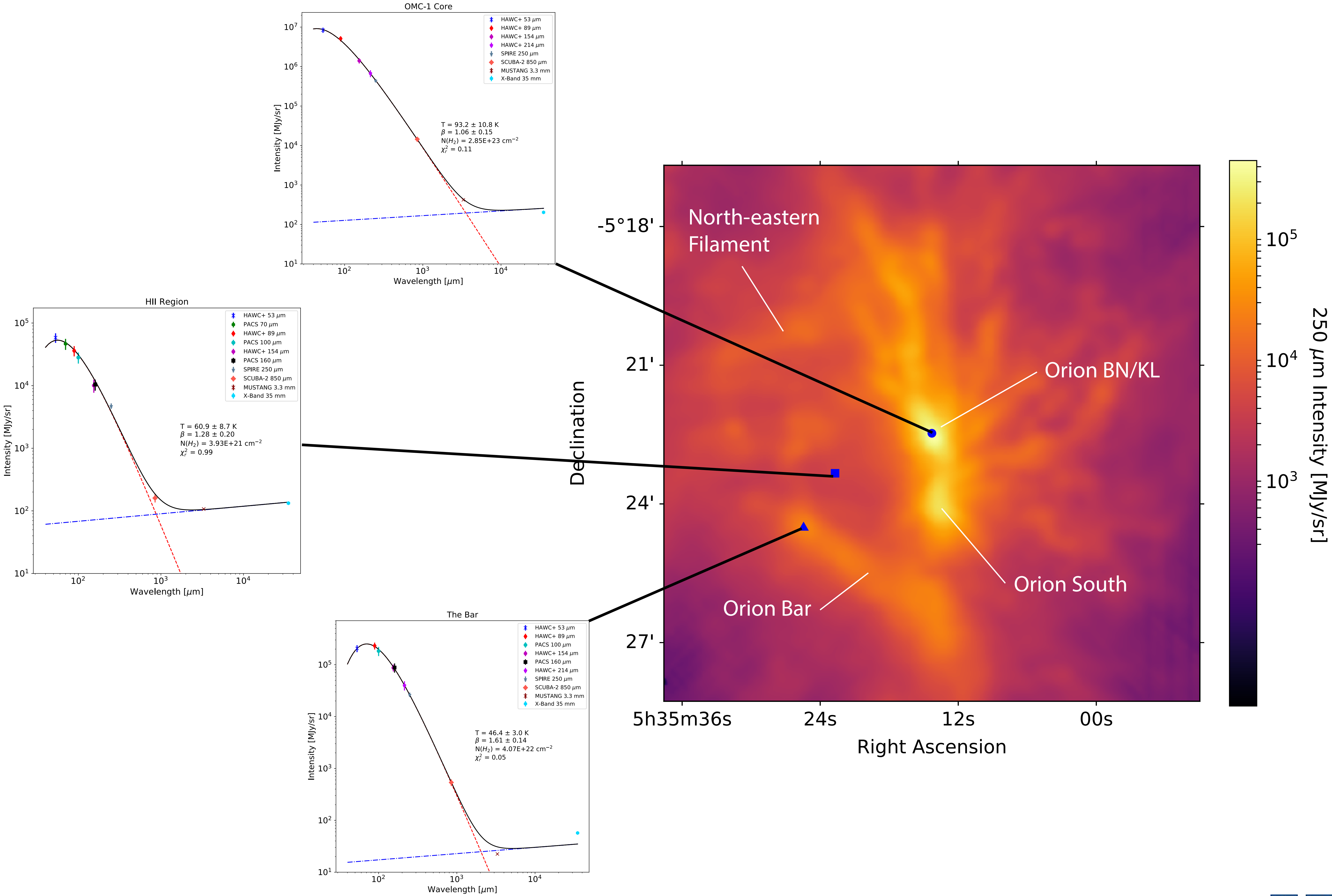
OMC-1 Core
HAWC+ 53 μm
HAWC+ 89 μm
HAWC+ 154 μm
HAWC+ 214 μm
SPIRE 250 μm
SCUBA-2 850 μm
MUSTANG 3.3 mm
X-Band 35 mm
T = 93.2 ± 10.8 K
β = 1.06 ± 0.15
N(H2) = 2.85E+23 cm−2
χr2 = 0.11
Intensity [MJy/sr]
Wavelength [μm]
HII Region
HAWC+ 53 μm
PACS 70 μm
HAWC+ 89 μm
PACS 100 μm
HAWC+ 154 μm
PACS 160 μm
SPIRE 250 μm
SCUBA-2 850 μm
MUSTANG 3.3 mm
X-Band 35 mm
T = 60.9 ± 8.7 K
β = 1.28 ± 0.20
N(H2) = 3.93E+21 cm−2
χr2 = 0.99
Intensity [MJy/sr]
Wavelength [μm]
The Bar
HAWC+ 53 μm
HAWC+ 89 μm
PACS 100 μm
HAWC+ 154 μm
PACS 160 μm
HAWC+ 214 μm
SPIRE 250 μm
SCUBA-2 850 μm
MUSTANG 3.3 mm
X-Band 35 mm
T = 46.4 ± 3.0 K
β = 1.61 ± 0.14
N(H2) = 4.07E+22 cm−2
χr2 = 0.05
Intensity [MJy/sr]
Wavelength [μm]
North-eastern
Filament
Orion BN/KL
Orion South
Orion Bar
-5°18'
21'
24'
27'
Declination
5h35m36s
24s
12s
00s
Right Ascension
250 μm Intensity [MJy/sr]

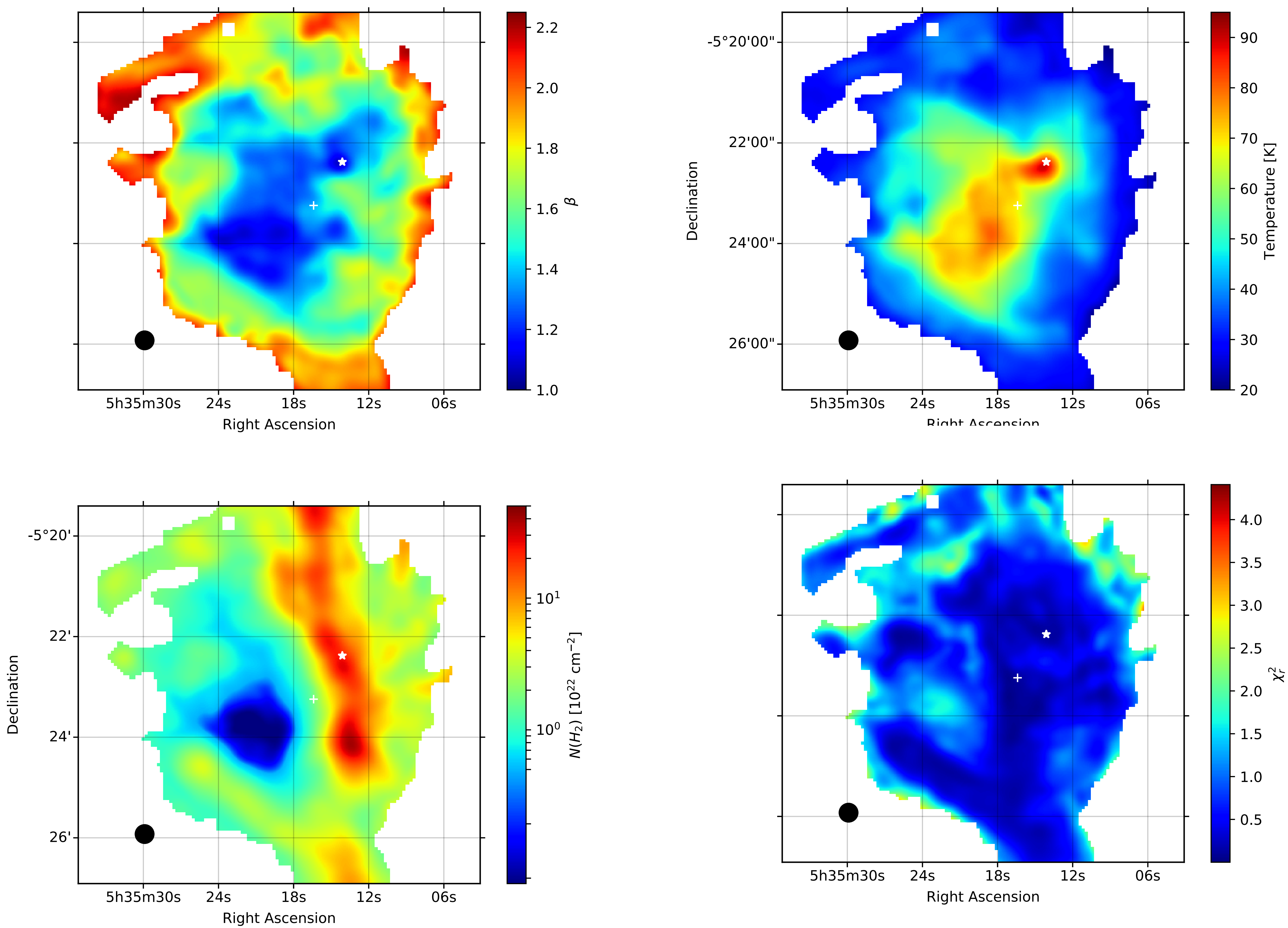
5h35m30s
24s
18s
12s
06s
Right Ascension
Declination
-5°20'00"
22'00"
24'00"
26'00"
-5°20'
22'
24'
26'
β
Temperature [K]
$N(H_2)$ [10^{22} cm^{-2}]
χ_r^2

T-beta correlation

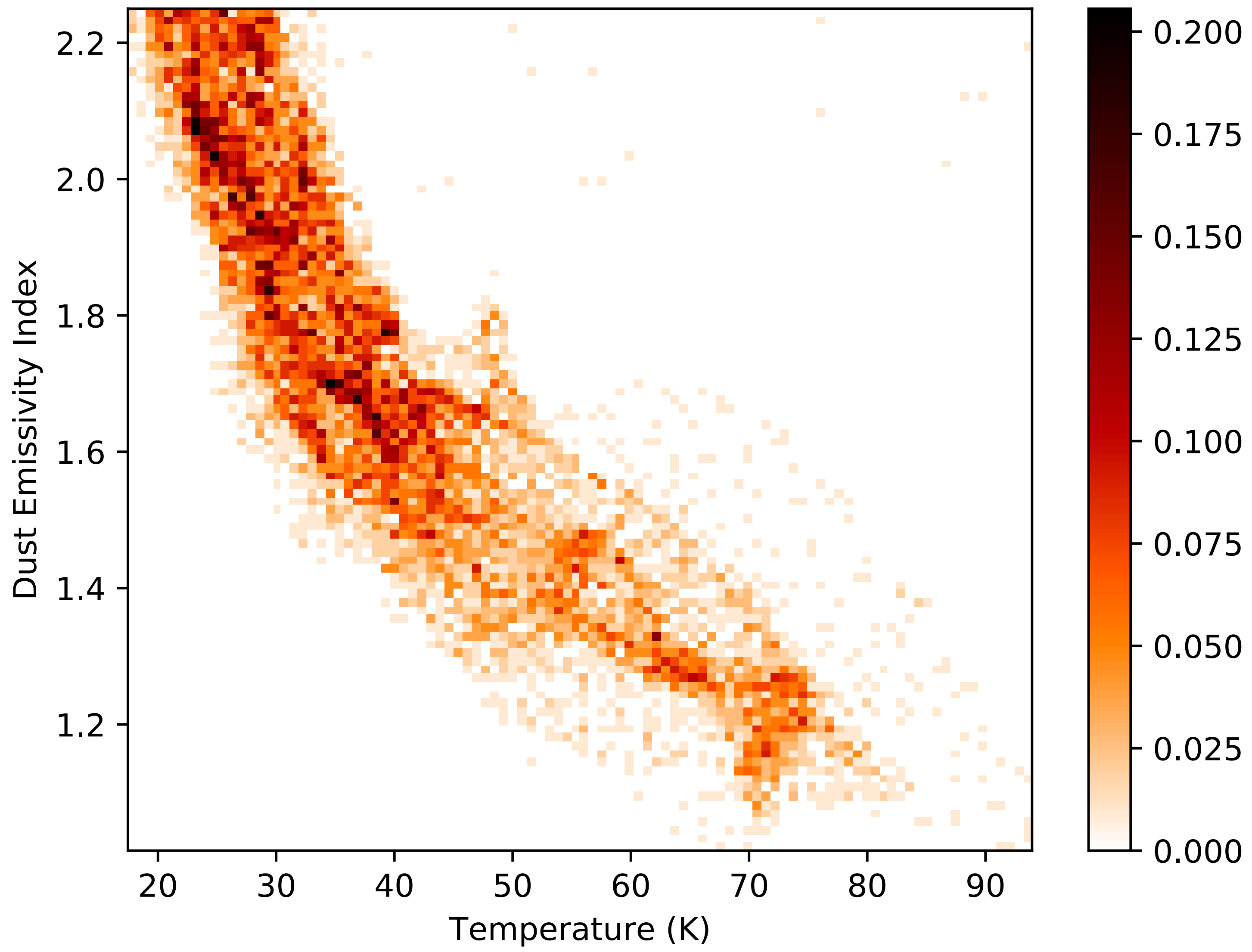

Dupac+ (2002,2003)- have seen this effect
Shetty+ (2009)- Suggest either line-of-sight variations or covariance due to noise in the fit

Is the T-beta correlation a systematic or physical ?

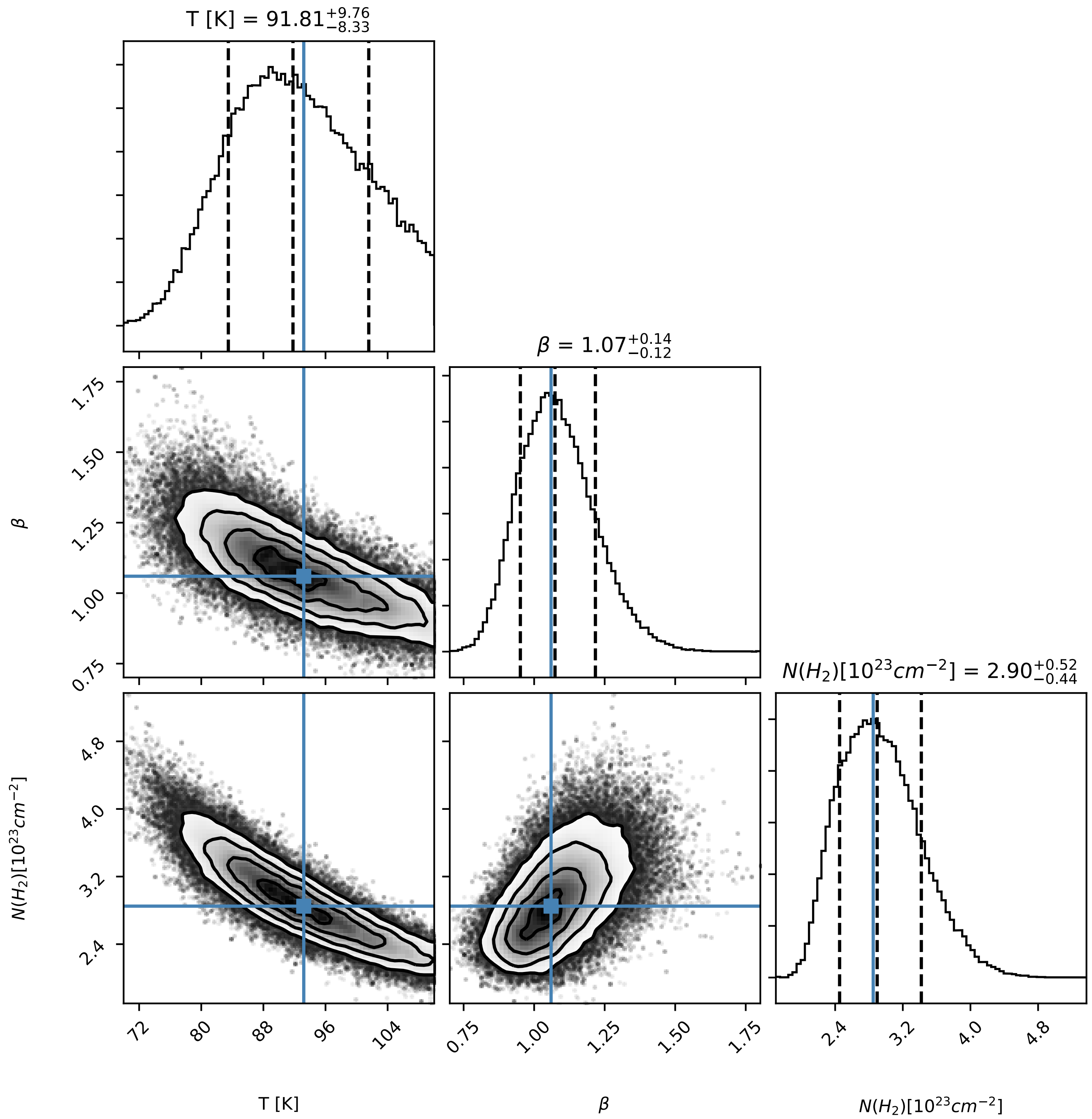

In agreement with Galametz+ (2012)

Polarization & Intensity

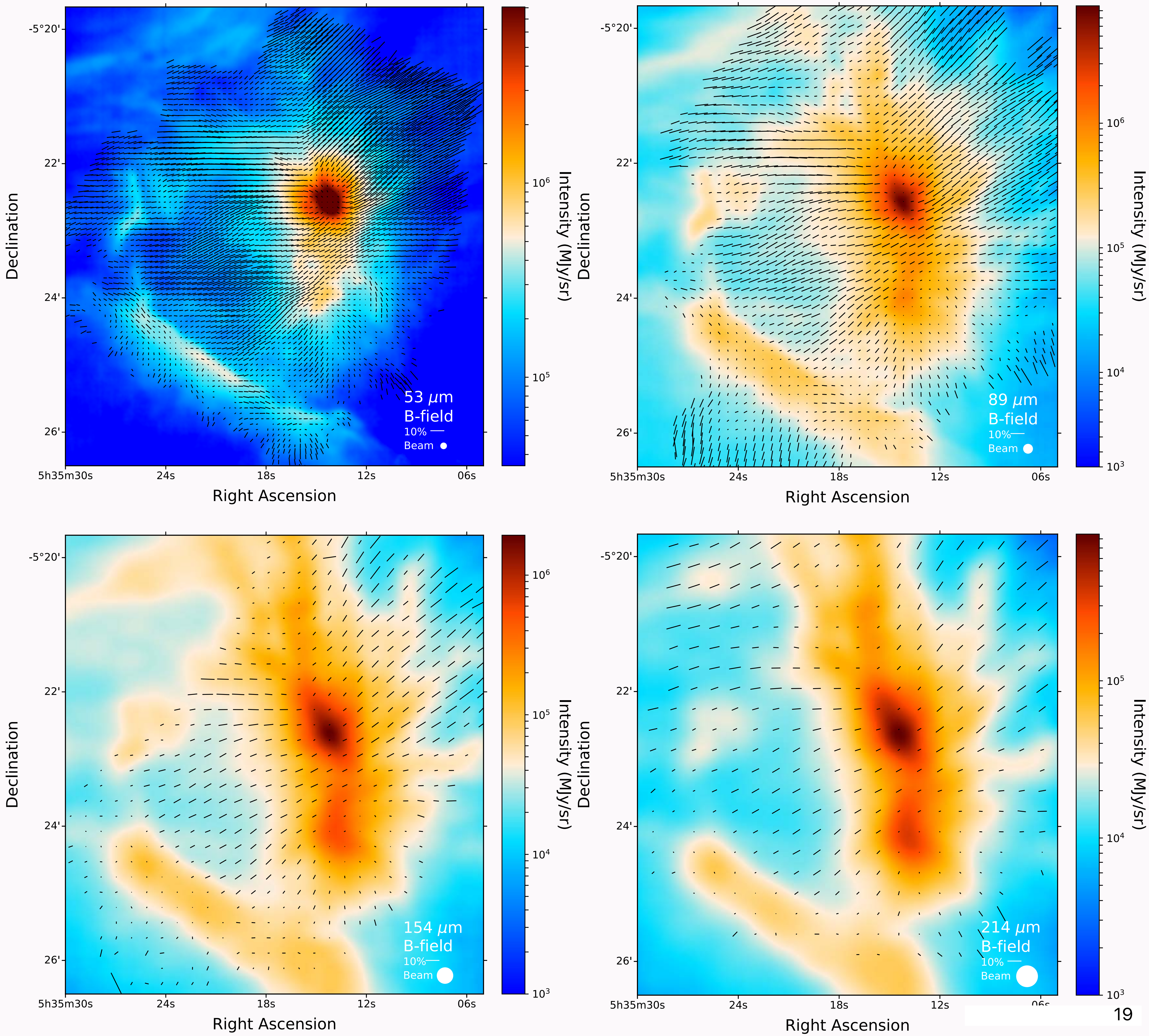

LIC & Intensity

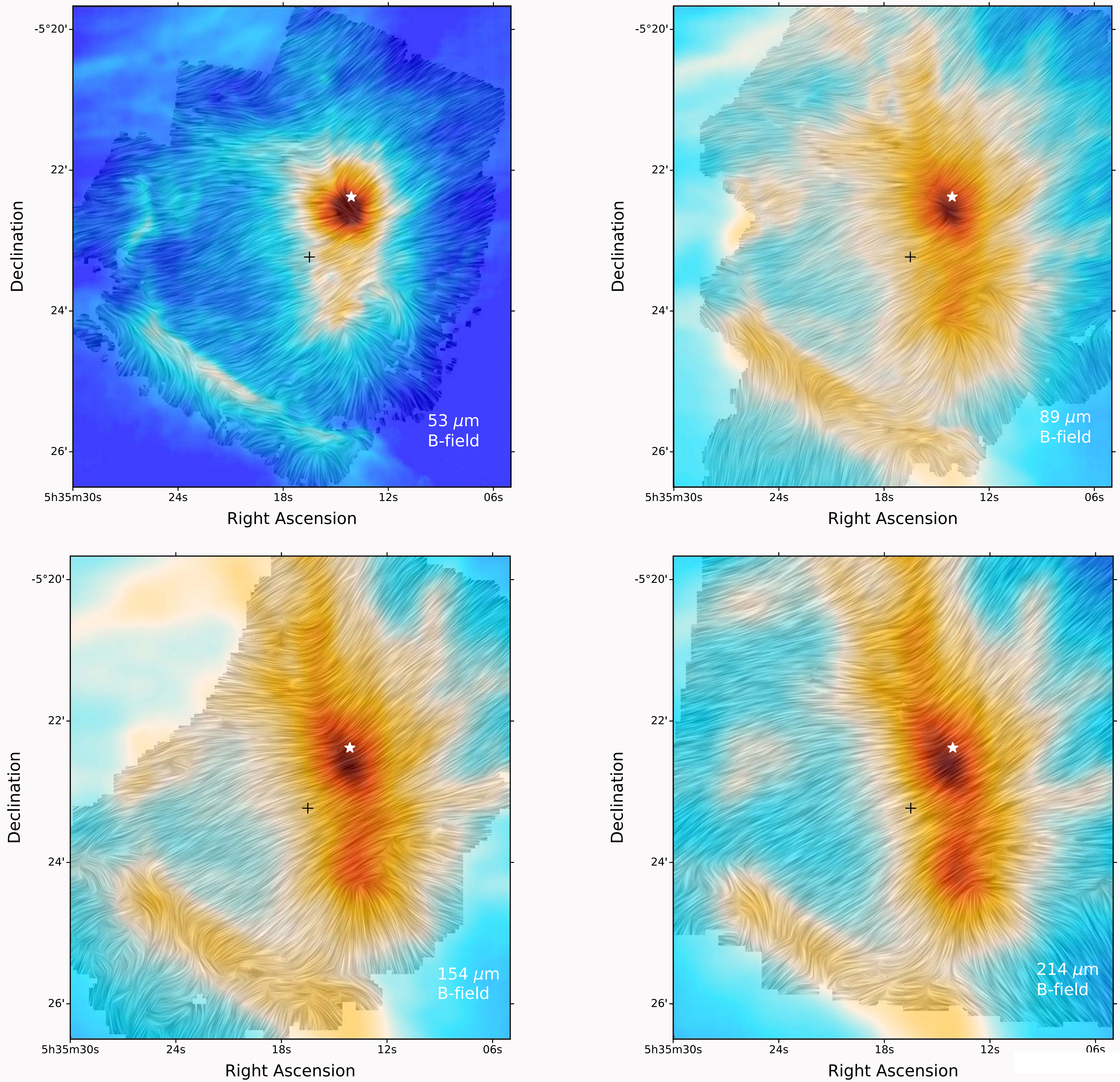

LIC: Leedom & Cabral (1994)

Polarized Intensity

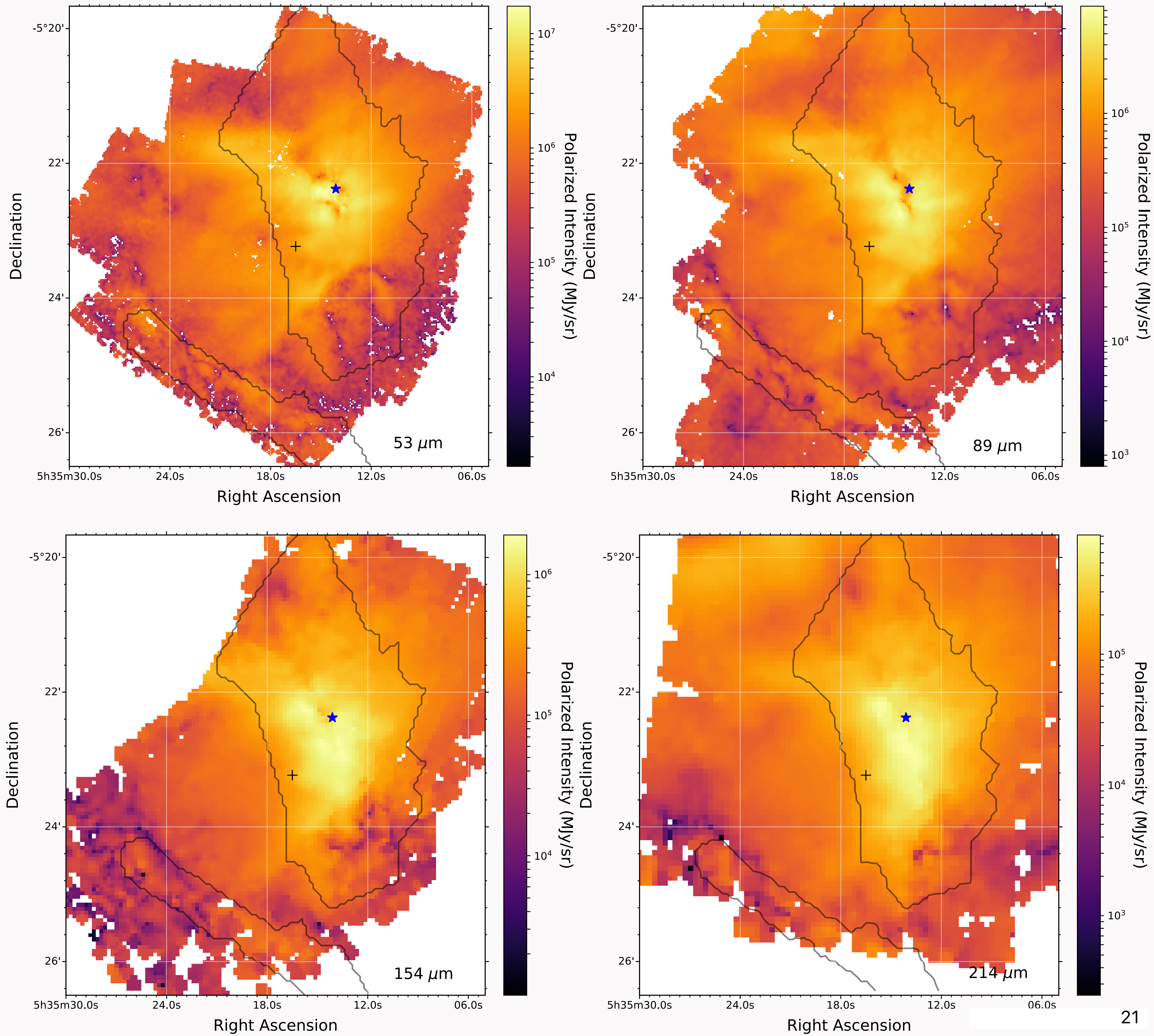

Thanks to Leslie Proudfit for putting this image together
NASA/SOFIA/D. Chuss+
VLT: ESO/M.

@MaeSocials
Feb 21
In response to
NASA tweet

Polarimetry Data Cuts

- Region Masks
- Accept only vectors with S/N>3
- Reference beam contamination

Regional Mask Definitions

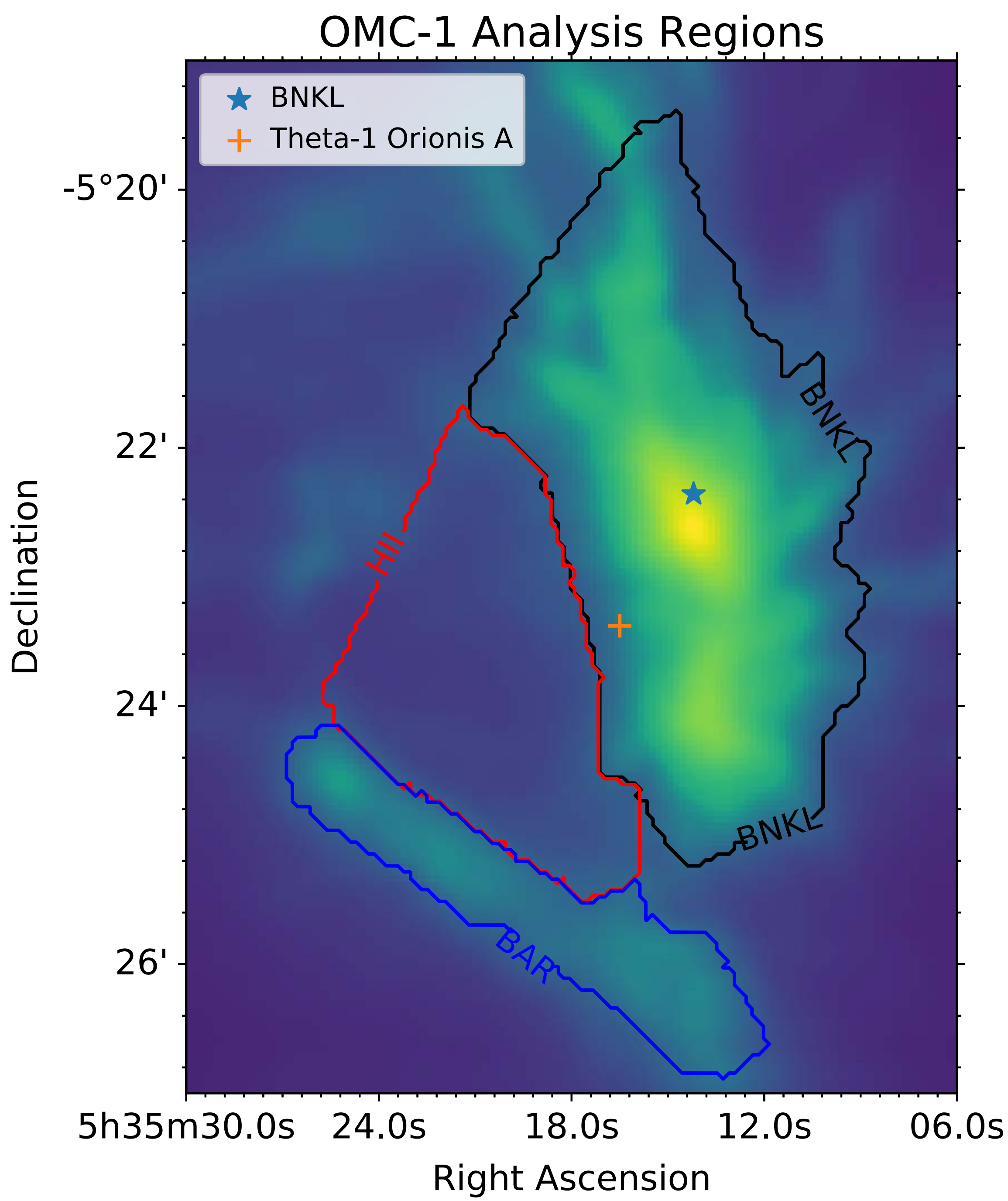

Reference Beam Contamination

Novak+ (1997) provide a technique for estimating the maximum possible systematic error from reference beam intensity
(assume reference beam is 10% contaminated)

$$w \equiv \bar{I}_r / I_m$$

$$p_{\rm sys}^{+} = \max\left[p_m, \left(\frac{p_m + p_r w}{1 + w}\right)\right],$$

$$p_{\rm sys}^{-} = \frac{p_m - p_r w}{1 + w},$$

$$\Delta\phi_{\rm sys} = \frac{1}{2}\arctan\left[\frac{p_r w}{(p_m^2 - p_r^2 w^2)^{1/2}}\right]$$

Reference Beam Contamination

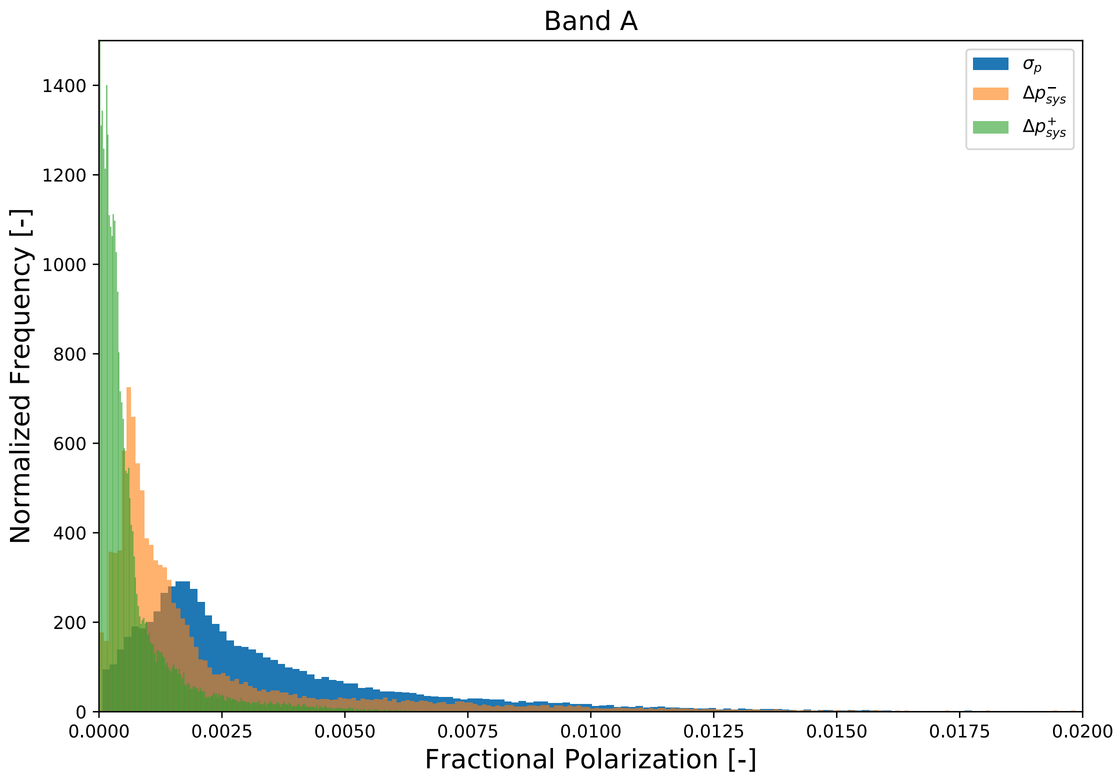

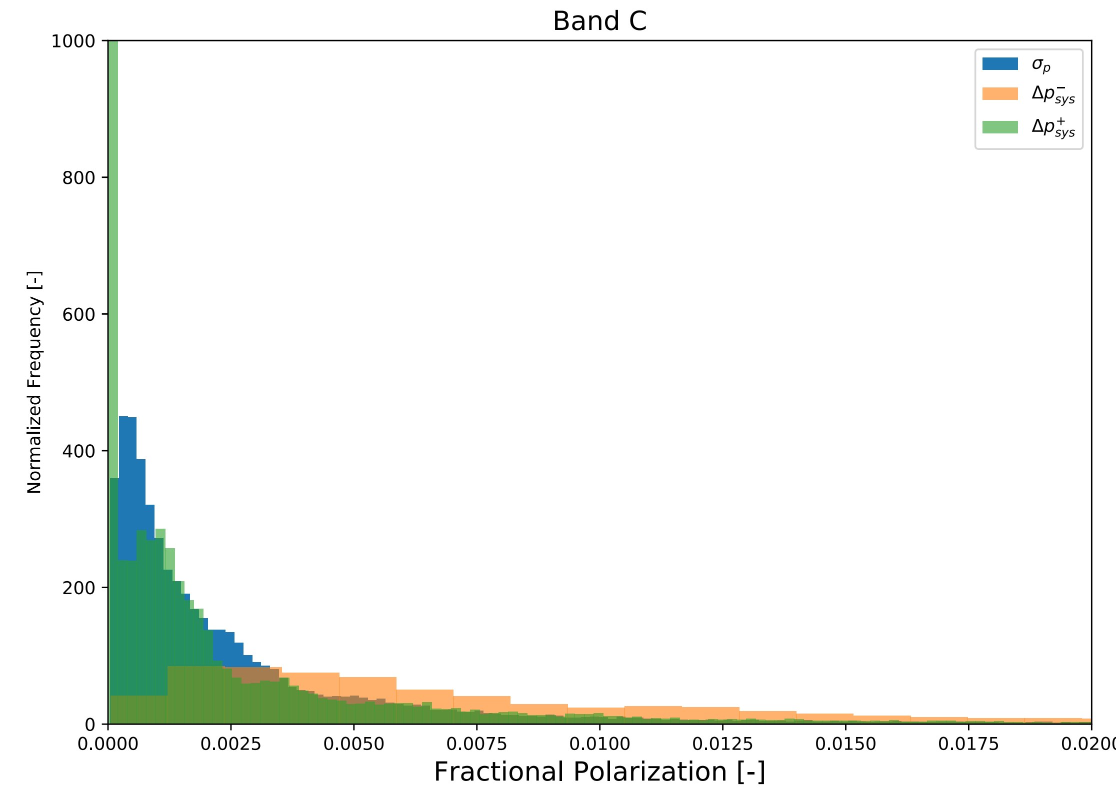

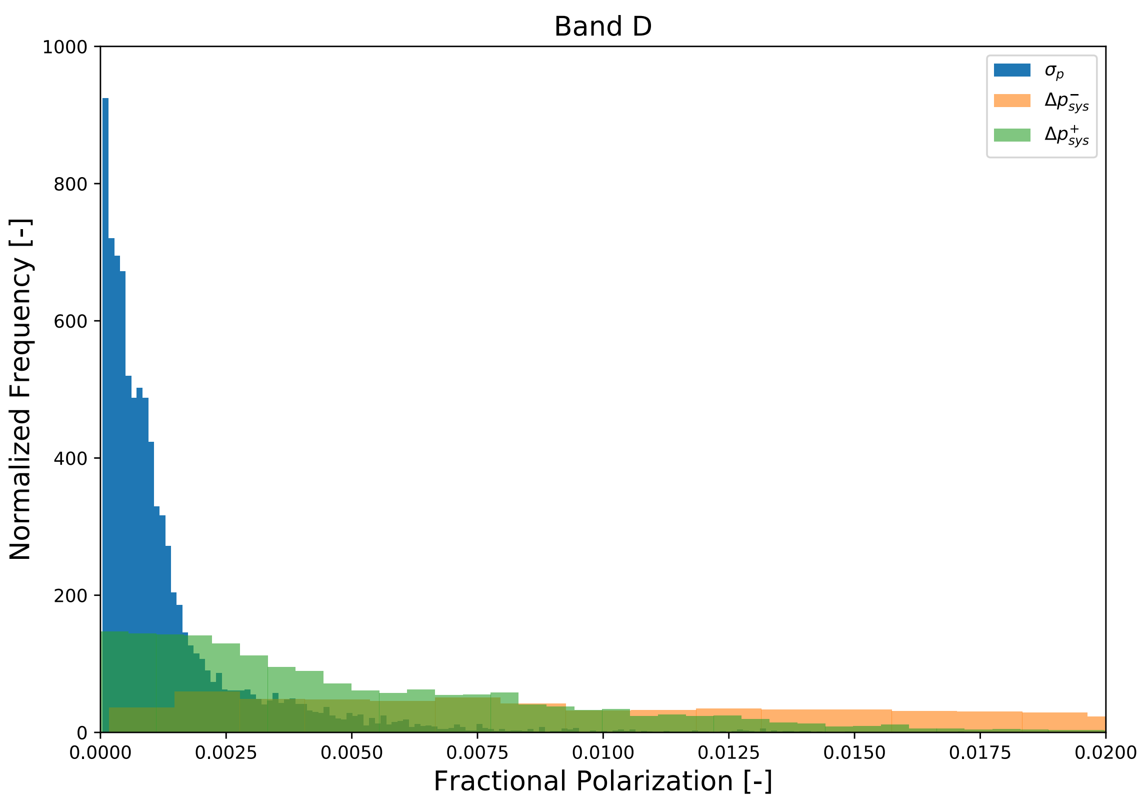

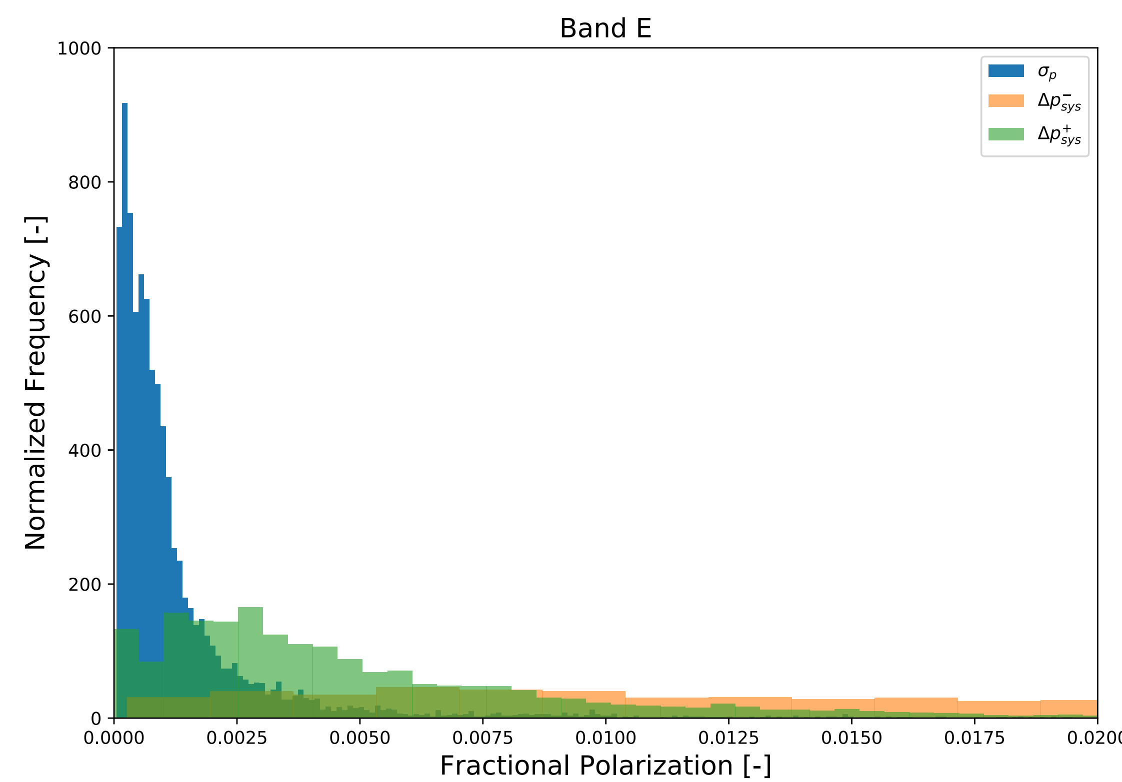

Systematic/Statistical Cuts

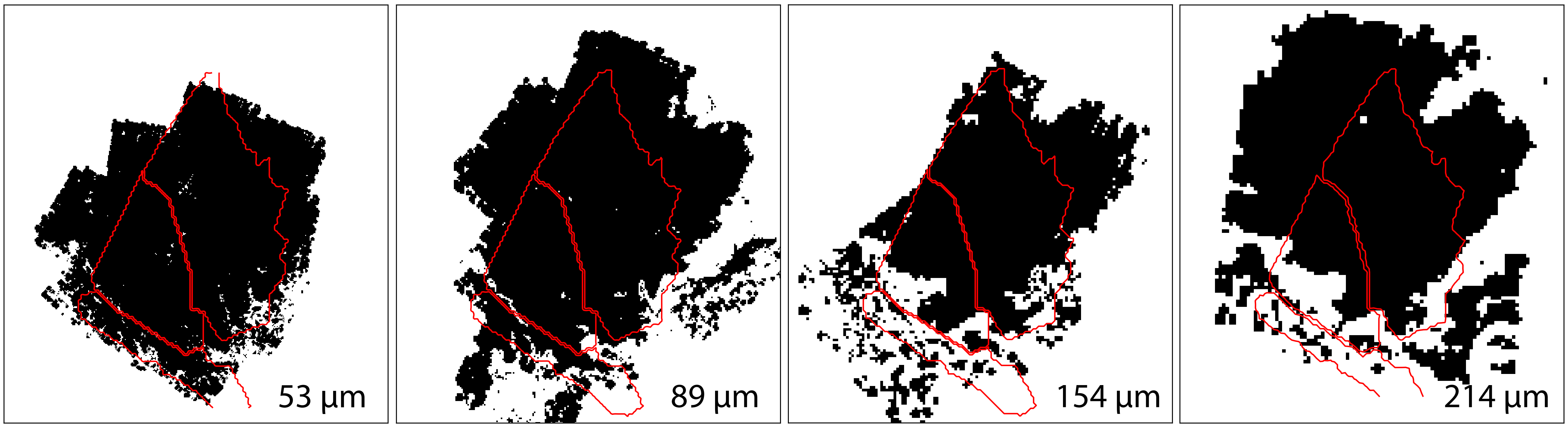

Example data cut masks: reference beam contamination contributes 10 deg or less of possible vector rotation (cut used for DCF)

Fractional Polarization v. Intensity

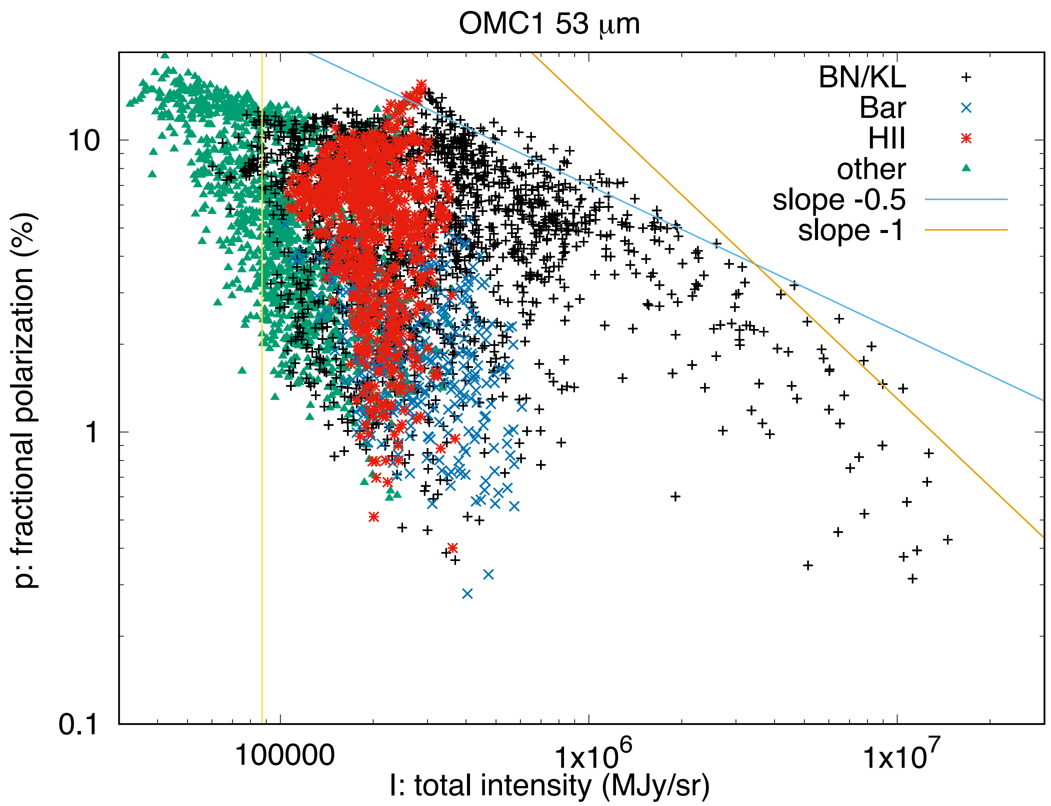

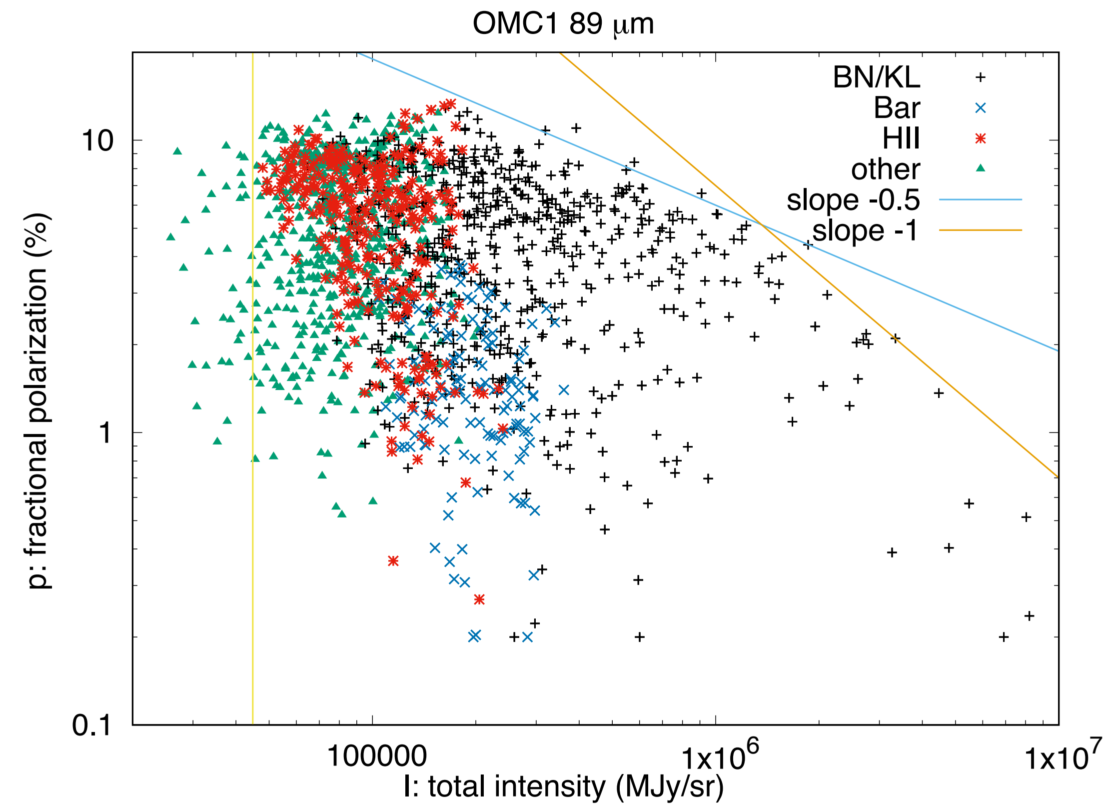

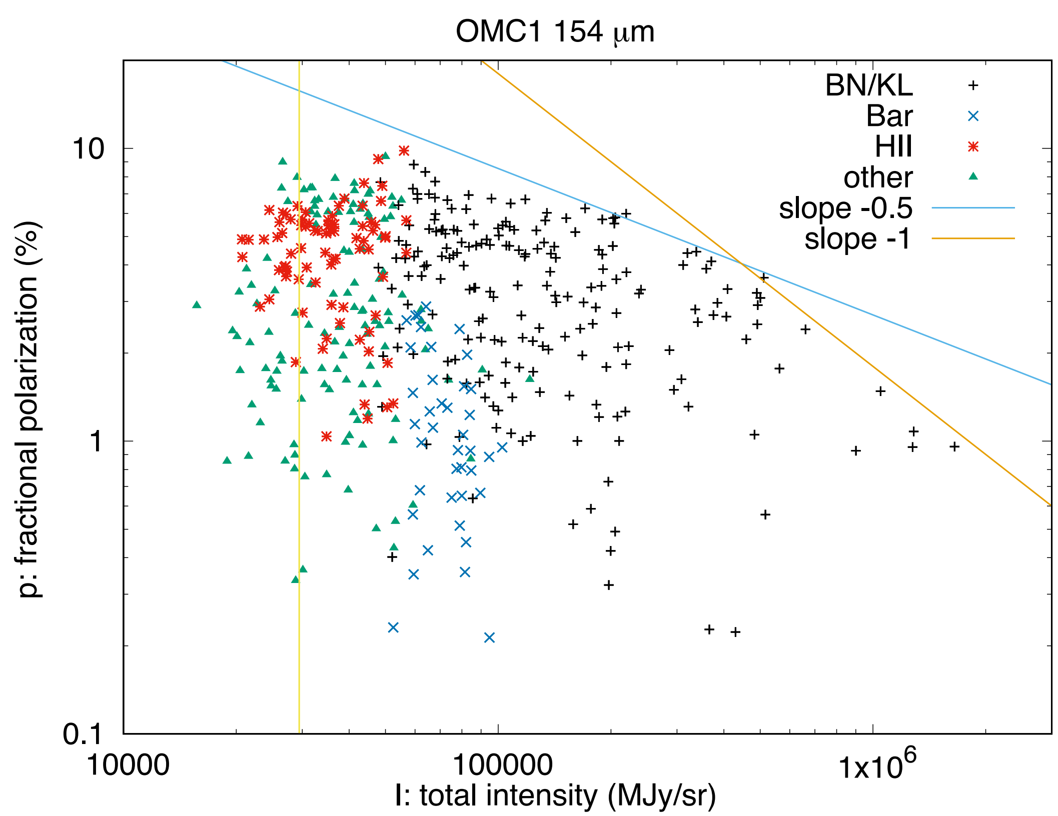

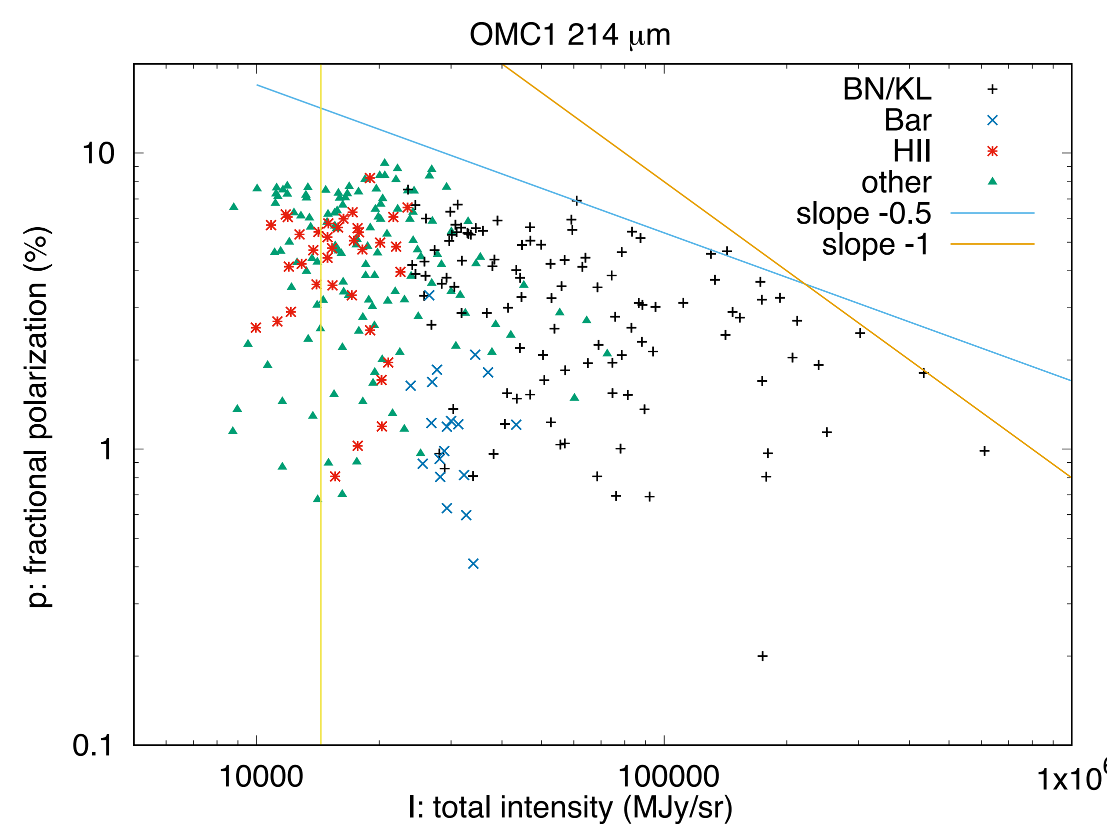

Possible causes for weak p, I anticorrelation

- Grain alignment is weaker in denser reasons (shielding of grains to ISRF)
- There is magnetic field structure on scales smaller than the beam
- Superposition of fields along the line of sight
- The magnetic field is oriented predominantly along the line of sight

Do the grains remain aligned in dense regions?

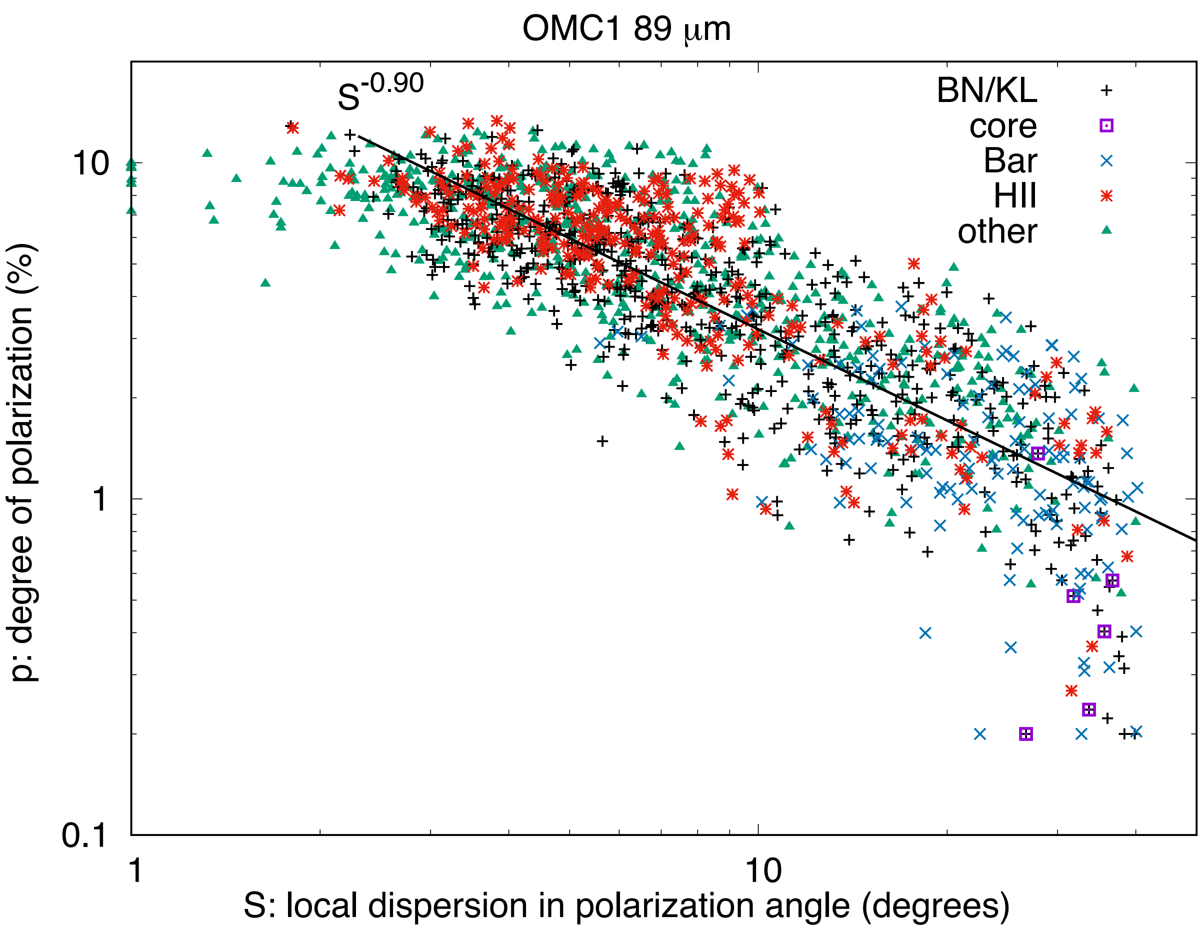

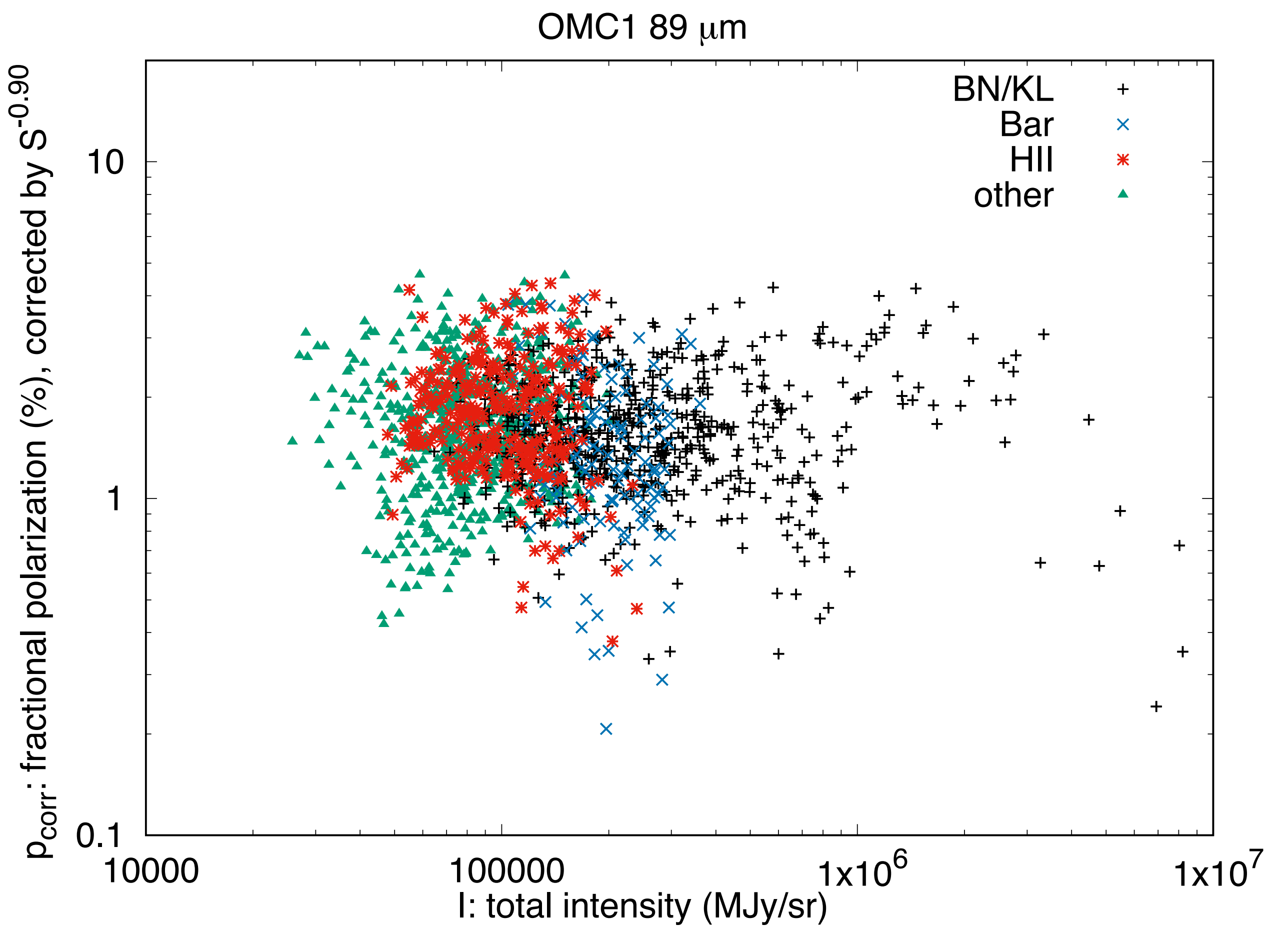

$$S = \sqrt{\langle (\phi - \overline{\phi})^2 \rangle} \approx \sqrt{\langle \sin^2(\phi - \overline{\phi}) \rangle}$$
$$= \sqrt{(1 - \langle \hat{q} \rangle \hat{q}(\overline{\phi}) - \langle \hat{u} \rangle \hat{u}(\overline{\phi}))/2},$$

$$p \approx p_0(I/\overline{I})^{\alpha_I}(S/\overline{S})^{\alpha_S}$$

Wavelength (μm)	θ_S (arcsec)	Best-Fit Trend
53	30	$p \approx 3.1\%(I/3.8 \times 10^5 MJy/sr)^{-0.01}(S/14.2^\circ)^{-0.87}$
89	30	$p \approx 2.6\%(I/2.4 \times 10^5 MJy/sr)^{-0.09}(S/12.5^\circ)^{-0.90}$
154	30	$p \approx 1.9\%(I/1.0 \times 10^5 MJy/sr)^{-0.19}(S/12.5^\circ)^{-0.84}$
214	30	$p \approx 2.3\%(I/0.42 \times 10^5 MJy/sr)^{-0.21}(S/8.6^\circ)^{-0.70}$

Fissel+ (2016) found evidence for loss of grain alignment in Vela C:

$$p \propto I^{-0.45}$$
$$p \propto S^{-0.60}$$

But, Vela C is 15 K, OMC-1 is 37 K, so much more (30x) radiation in OMC-1 cores (perhaps due to embedded stars)

Davis-Chandrasekhar-Fermi: Estimating the Magnetic Field Strength

- DCF [Davis (1951); Chandrasekhar & Fermi (1953)] equate the kinetic energy from turbulence with the dispersion in the polarization vectors (magnetic field) to estimate the magnetic field strength.
- Issue: The large scale field can masquerade as “turbulence” in the simple picture.
- Houde+ (2009, 2011, 2016) Use the dispersion function (2 point correlation of field directions) to fit out the large scale field and marginalize over variations within the beam column.

$$1 - \langle \cos[\Delta\phi(l)] \rangle = \frac{1}{1 + \mathcal{N}\left[\frac{\langle B_t^2 \rangle}{\langle B_0^2 \rangle}\right]^{-1}} \left\{1 - \exp\left(-\frac{l^2}{2(\delta^2 + 2W^2)}\right)\right\} + a_2 l^2$$

$$\mathcal{N} = \frac{(\delta^2 + 2W^2)\Delta'}{\sqrt{2\pi}\,\delta^3}.$$

$$\Delta'' \equiv \Delta' \left(\frac{\langle B_t^2 \rangle}{\langle B_0^2 \rangle}\right)^{-1}$$

Define this parameter because of degeneracy between parameters

Davis-Chandrasekhar-Fermi: Estimating the Magnetic Field Strength

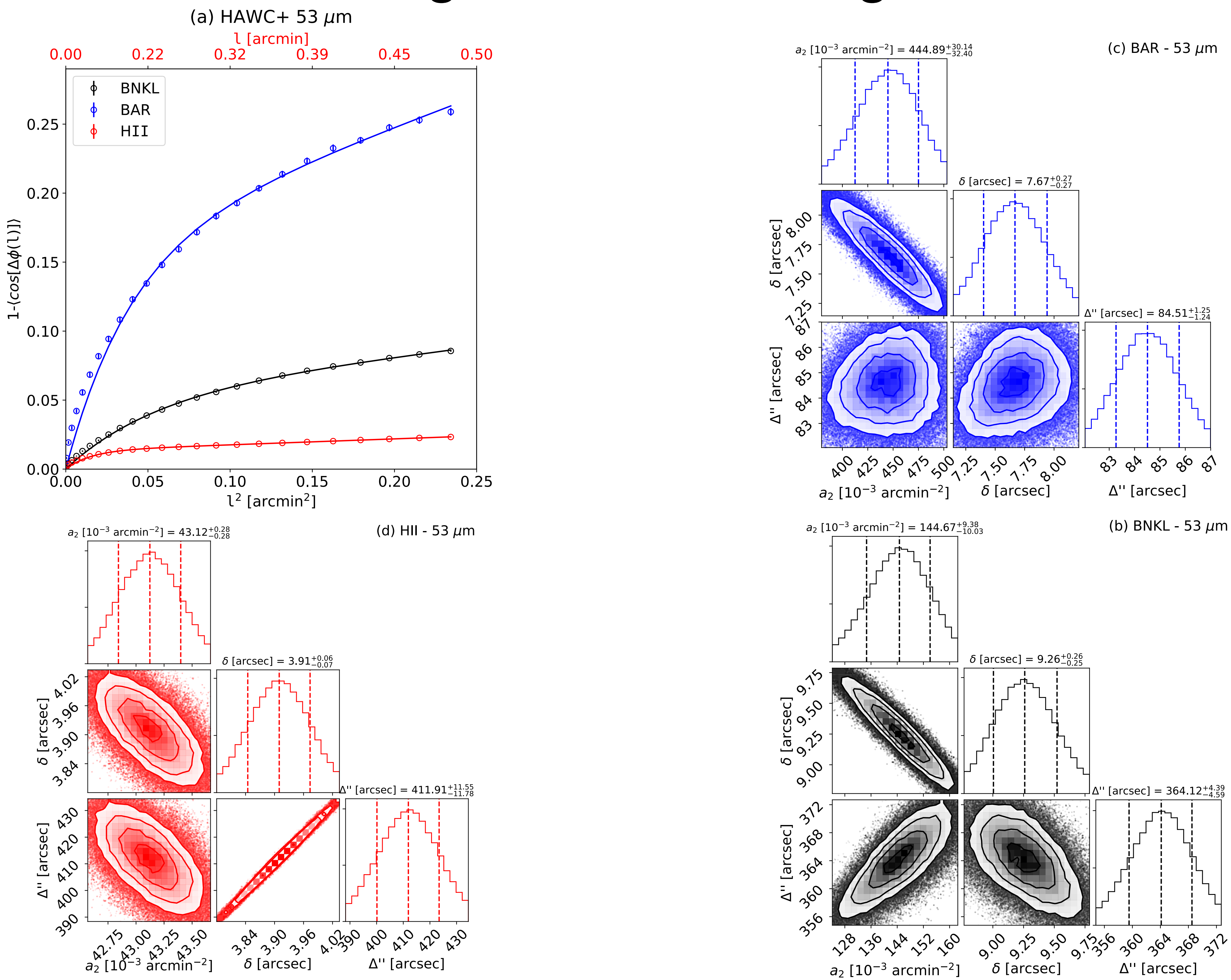

Wavelength $[\mu m]$	a_2 $[10^{-3}\ \mathrm{arcmin}^{-2}]$	δ [arcsec]	Δ'' [arcsec]
BNKL			
53	$144.67^{+9.38}_{-10.03}$	$9.26^{+0.26}_{-0.25}$	$364.12^{+4.39}_{-4.59}$
89	$74.34^{+1.92}_{-1.95}$	$10.26^{+0.30}_{-0.30}$	$387.36^{+9.41}_{-9.85}$
154	$36.02^{+3.34}_{-3.70}$	$21.69^{+1.79}_{-1.67}$	$622.90^{+23.16}_{-22.55}$
214	$7.15^{+3.25}_{-3.47}$	$33.85^{+2.68}_{-2.61}$	$707.10^{+30.59}_{-30.76}$
BAR			
53	$444.89^{+30.14}_{-32.40}$	$7.67^{+0.27}_{-0.27}$	$84.51^{+1.25}_{-1.24}$
89	$158.65^{+8.59}_{-8.69}$	$10.24^{+0.21}_{-0.20}$	$94.74^{+1.08}_{-1.09}$
154	–	–	–
214	–	–	–
HII			
53	$43.12^{+0.28}_{-0.28}$	$3.91^{+0.06}_{-0.07}$	$411.91^{+11.5}_{-11.78}$
89	$18.85^{+1.48}_{-1.55}$	$9.29^{+0.57}_{-0.57}$	$744.77^{+46.93}_{-50.14}$
154	$12.60^{+0.73}_{-0.73}$	$9.37^{+0.42}_{-0.59}$	$941.24^{+43.67}_{-95.68}$
214	$14.78^{+0.73}_{-0.74}$	$10.20^{+0.61}_{-1.09}$	$888.12^{+82.86}_{-174.00}$

$$B_0 \simeq \sqrt{4\pi\rho}\sigma(v)\left[\frac{\langle B_t^2\rangle}{\langle B_0^2\rangle}\right]^{-1/2} = \sqrt{4\pi\rho}\sigma(v)\left[\frac{\Delta'}{\Delta''}\right]^{-1/2}$$

Wavelength [μm]	$N(H_2)$ [cm^{-2}]	$\frac{\langle B_t^2\rangle}{\langle B_0^2\rangle}$	B_0 [μG]	$\mathcal{N}$
BNKL				
53	$(9.85\pm8.96)\times10^{22}$	0.37	1002	6.67
89	...	0.43	931	8.42
154	...	0.37	1013	5.02
214	...	0.42	944	4.02
BAR				
53	$(3.87\pm2.12)\times10^{22}$	1.61	303	8.50
89	...	1.77	289	8.44
154	...	–	–	
214	...	–	–	
HII				
53	$(5.90\pm3.24)\times10^{21}$	0.33	261	24.59
89	...	0.23	316	9.76
154	...	0.24	305	19.32
214	...	0.34	259	30.23

The BN/KL Explosion: Magnetic Implications

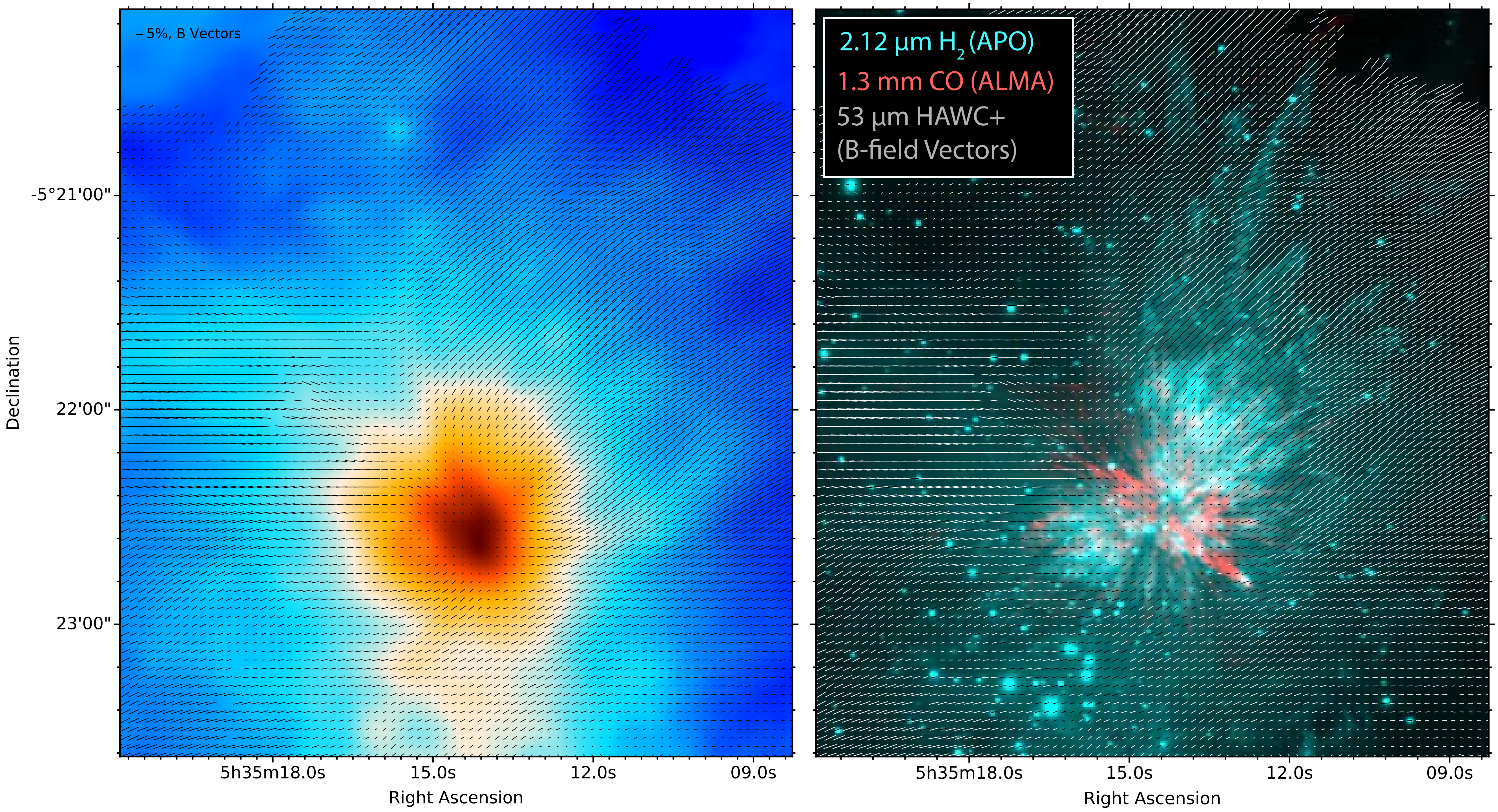

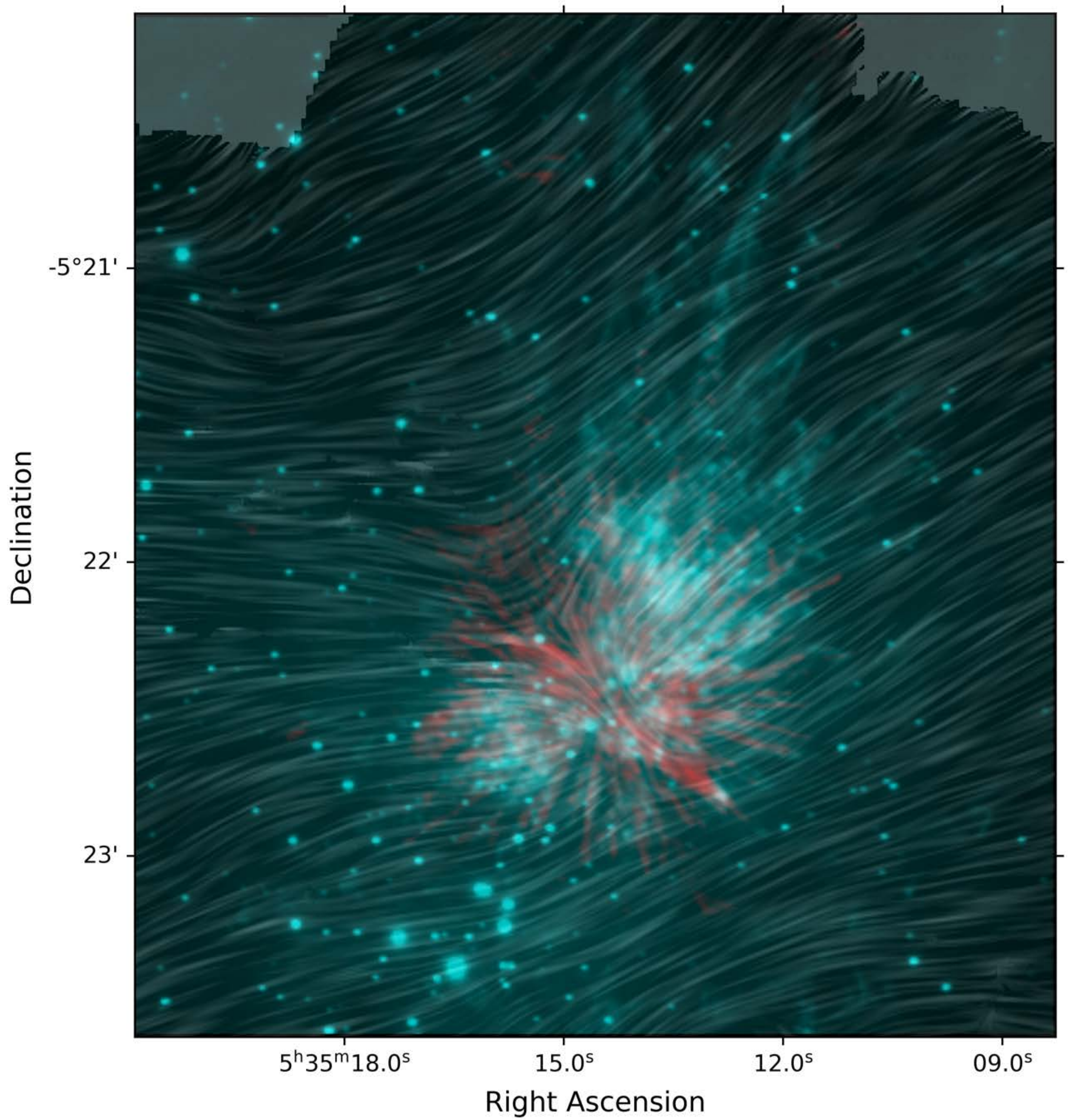

-5°21'
22'
23'
Declination
5h35m18.0s
15.0s
12.0s
09.0s
Right Ascension

The BN/KL Explosion: Magnetic Implications

Inner Part of the Explosion (corresponding to ~isotropic CO fingers)

$$B_{\rm crit} = \sqrt{8\pi u_M} = 14.4\left(\frac{D}{400\,{\rm pc}}\right)^{-3/2}\left(\frac{\theta}{30''}\right)^{-3/2}\left(\frac{E}{2\times10^{47}\,{\rm ergs}}\right)^{1/2}\ {\rm mG}.$$

Outer Part of the Explosion (corresponding to bipolar H2 fingers)

$$B_{\rm crit} = 0.6\left(\frac{D}{400\,{\rm pc}}\right)^{-3/2}\left(\frac{\theta_R}{30''}\right)^{-1}\left(\frac{\theta_H}{230''}\right)^{-1/2}\left(\frac{E}{2\times10^{45}\,{\rm ergs}}\right)^{1/2}\ {\rm mG}.$$

From the DCF analysis, B~1.0 mG.
Therefore, we expect the magnetic field to be subdominant to the kinetic energy density near the center, but dominate farther out.

Conclusions

- New maps of temperature and col. Density
- Magnetic field structure of OMC-1 is indicative of Magnetically-regulated star formation, but also traces the dynamics of the region
- No evidence for decreased grain alignment in cloud cores
- Magnetic field strength estimates: 1 mG in BN/KL regions, ~300 microgauss elsewhere.

Software Acknowledgments

- python, Ipython (Pérez & Granger 2007)
- numpy (van der Walt et al. 2011)
- scipy (Jones et al. 2001) matplotlib (Hunter 2007)
- emcee (Foreman-Mackey et al. 2013)
- corner (Foreman-Mackey 2016)
- astropy (Astropy Collaboration et al. 2013; Price-Whelan et al. 2018)
- LIC code (ported from public available IDL source by Diego Falceta-Gonçalves).